PI(4,5)P2 triggers activation of Focal Adhesion Kinase by inducing clustering and conformational changes.

Guillermina M. Goñi[1], Carolina Epifano[2], Jasminka Boskovic[1], Marta Camacho-Artacho[1], Jing Zhou[3], Agnieszka K. Bronowska[3], M. Teresa Martín[4], Michael J. Eck[5,6], Leonor Kremer[4], Frauke Gräter[3], Francesco L. Gervasio[7], Mirna Perez-Moreno[2], and Daniel Lietha[1*]

[1] Structural Biology and Biocomputing Programme, [2] BBVA Foundation – CNIO Cancer Cell Biology Programme, Spanish National Cancer Research Centre (CNIO), Madrid 28029, Spain [3] Heidelberg Institute for Theoretical Studies (HITS), Heidelberg 69118, Germany [4] Immunology and Oncology Department, Centro Nacional de Biotecnología, Consejo Superior de Investigaciones Científicas (CNB-CSIC), Madrid 28049, Spain [5] Department of Biological Chemistry and Molecular Pharmacology, Harvard Medical School, Boston, MA 02115, USA [6] Department of Cancer Biology, Dana-Farber Cancer Institute, Boston, MA 02115, USA [7]Department of Chemistry and Institute of Structural Molecular Biology, University College London, London, UK

Submitted to Proceedings of the National Academy of Sciences of the United States of America

Focal adhesion kinase (FAK) is a non-receptor tyrosine kinase (NRTK) with key roles in integrating growth and cell-matrix adhesion signals and in cancer FAK is a major driver of invasion and metastasis. Cell adhesion via integrin receptors is well known to trigger FAK signaling and many of the players involved are known, however, mechanistically FAK activation is not understood. Here, using a multidisciplinary approach including biochemical, biophysical, structural, computational and cell biology approaches, we provide a detailed view of a multistep activation mechanism of FAK initiated by the phosphoinositide PI(4,5)P2. Interestingly, the mechanism differs from canonical NRTK activation and is tailored to the dual catalytic and scaffolding function of FAK. We find PI(4,5)P2 induces clustering of FAK on the lipid bilayer by binding a basic region in the regulatory FERM domain. In these clusters PI(4,5)P2 induces a partially open FAK conformation where the autophosphorylation site is exposed, facilitating efficient autophosphorylation and subsequent Src recruitment. However, PI(4,5)P2 does not release autoinhibitory interactions, but rather Src phosphorylation of the activation loop in the FAK kinase results in release of the FERM/kinase tether and full catalytic activation. We propose that PI(4,5)P2 and the enzyme generating it in focal adhesions (PIP5KIγ) are important in linking integrin signaling to FAK activation.

Focal Adhesion Kinase | Phosphoinositide | Cell Signaling

INTRODUCTION

Cell attachment to the extracellular matrix (ECM) is mediated via integrin transmembrane receptors on the cell surface. Integrin engagement to ECM components results in activation and clustering of integrins. In response to integrin activation, a large number of proteins are recruited to their cytoplasmic tails, resulting in the formation of focal adhesions (FAs) (1). On the one side FAs are anchoring points for actomyosin stress fibers, which allow tension forces to build up when contracting fibers exert their pulling force via FAs against the ECM. On the other hand integrin activation and the generation of tension, triggers intricate signaling cascades. A central signaling component in FAs is the non-receptor tyrosine kinase focal adhesion kinase (FAK). FAK is activated downstream of integrins and its signaling is important for cell migration, proliferation and survival (2, 3). FAK contains numerous binding sites for other signaling and adaptor proteins and has been identified as a hub in the FA interactome (4). In addition to its role as a signaling kinase, FAK is therefore also thought to function as a signaling scaffold. FAK is required for diverse processes in development, wound healing and disease (5-7). FAK knockout mice are not viable due to mesodermal defects (8), and early studies with FAK knockout cells indicated that FAK is important in FA turnover by inhibiting Rho activity (9, 10). Subsequent studies portray a more complex picture (11) and indicate that FAK is also involved in increasing adhesion strength, in particular in response to tension forces (12, 13). FAK is frequently overexpressed in various human cancers (14). Its overexpression highly correlates with tumor invasiveness, hence FAK is widely pursued as a drug target for cancer therapy (15, 16).

FAK is a 120 kDa multidomain protein containing an N-terminal FERM (4.1, ezrin, radixin, moesin homology) domain, followed by a 50 residue linker, a central kinase domain, a ~220 residue low complexity proline-rich region, and a C-terminal FA targeting (FAT) domain (Fig. 1A). Whereas the FAT domain is important for targeting FAK to FAs through interactions with paxillin (17-19), the FERM domain is responsible for regulating catalytic activity (20). In the autoinhibited state the FERM domain docks onto the kinase domain, which results in catalytic inhibition and sequesters regulatory phosphorylation sites (21). FAK activation initially results in autophosphorylation of Y397 in the linker between the FERM and kinase domains (22), a process reported to occur in *trans* (23). Phosphorylated Y397 provides a docking site for the SH2 domain of the Src kinase and recruited Src phosphorylates several tyrosines in FAK. Two of them (Y576 and Y577) are located in the activation loop of the FAK kinase and their phosphorylation confer full catalytic activity (24). The activated FAK/Src complex phosphorylates several FA proteins, including paxillin (25) and p130Cas (26).

Significance

Non receptor tyrosine kinases (NRTKs) are major players in cell signaling. Among them, FAK is the key integrator of signals from growth factors and cell adhesion. In cancer FAK is frequently overexpressed and by promoting adhesion to the tumor stroma and extracellular matrix FAK provides important signals for tumor invasion and metastasis. Although autoinhibitory mechanisms have previously been described and the players involved in FAK regulation are largely known, on a mechanistic level FAK activation is currently not understood. Here we present a multidisciplinary approach demonstrating a multistep mechanism resulting in FAK activation. This new insight opens novel strategies to design potential anti-cancer drugs that inhibit both, catalytic and scaffolding functions of FAK with high specificity.

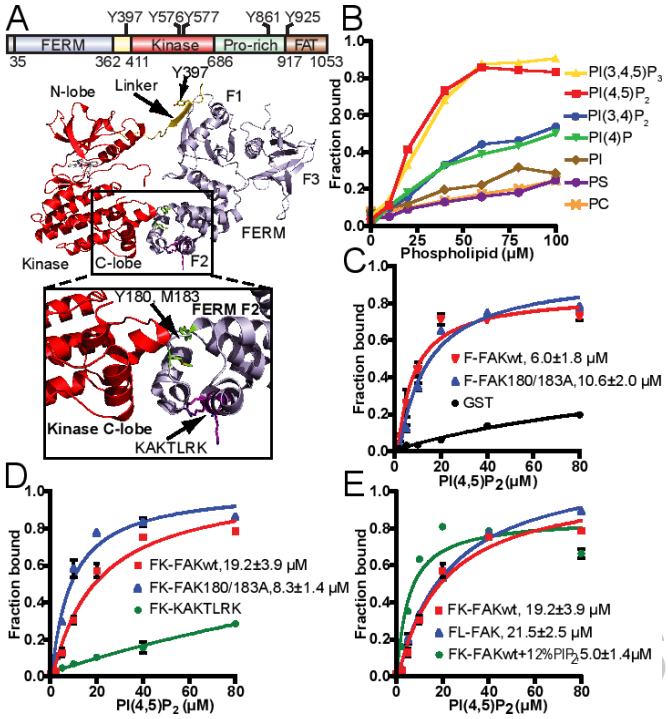

Fig. 1. FAK specifically interacts with PI(4,5)P_2 via the basic patch in the FERM domain. *(A)*Domain structure of FAK with the main phosphorylation sites indicated and ribbon diagram of the FK-FAK (FERM+Kinase) crystal structure as reported in (21) (pdb 2j0j). In the zoom window, the interaction between the FERM F2-lobe and the kinase C-lobe is shown, with residues Y180 and M183 at the interface colored in green and the basic KAKTLRK residues K216, K218, R221 and K222 in magenta. *(B)* The lipid binding specificity of FK-FAK was studied using vesicle pulldown assays with phosphatidyl choline (PC) vesicles containing 6% (mol/mol) of the indicated phospholipids. Phosphorylation of the D4 and D5 position of the inositol headgroup confer full binding affinity. (PI=phosphatidyl inositol; PS=phosphatidyl serine). *(C)* Vesicle pulldowns with 6% (mol/mol) PI(4,5)P_2 vesicles and GST fused F-FAKwt (FERM=FAK31-405) or F-FAK180/183A (Y180 and M183 mutated to alanine). The mutations do not affect PI(4,5)P_2 binding. GST fusions were used in order to obtain higher readouts (see methods section). *(D)* PI(4,5)P_2 vesicle pulldowns with FK-FAKwt, FK-FAK180/183A or FK-FAK-KAKTLRK (all KAKTLRK basic residues are mutated to alanine). Y180/M183A mutations result in approximately 2.5 fold higher affinity to PI(4,5)P_2 whereas the KAKTLRK mutations abolish binding *(E)* Vesicle pulldowns with 6% (mol/mol) PI(4,5)P_2 and FL-FAK reveals similar PI(4,5)P_2 affinity as for FK-FAKwt. Increasing the PI(4,5)P_2 density to 12% (mol/mol) results in approximately 4 fold higher affinity for FK-FAKwt. *(C-E)* Error bars represent SD from three independent experiments and are shown if larger than the symbol. Kd's are determined by fitting a one site binding model.

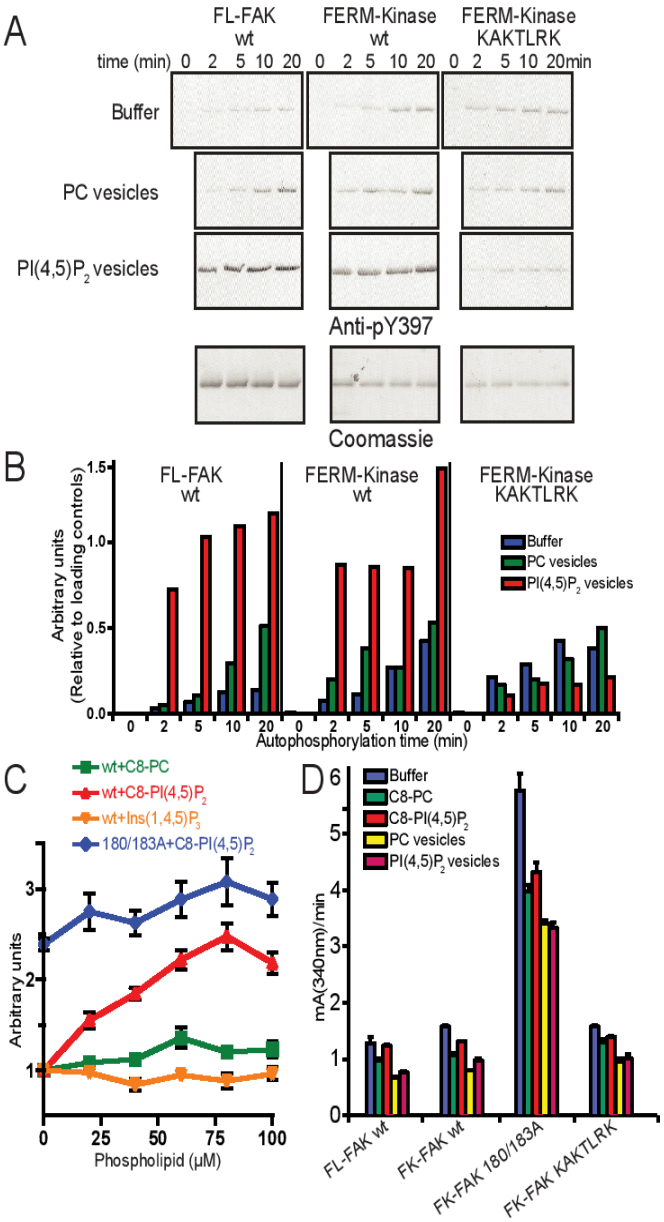

Fig. 2. PI(4,5)P_2 mediates FAK autophosphorylation but not catalytic turnover. *(A)* An autophosphorylation time course of FL-FAK, FK-FAKwt and FK-FAK-KAKTLRK in the absence (Buffer) or presence of PI(4,5)P_2 or PC vesicles was monitored by immuno blotting, using an anti-pY397 antibody. The bottom panels are loading controls stained by Coomassie. Note that FL-FAK stains stronger because of its larger molecular weight. *(B)* Quantifications of blots from (A) relative to loading controls (using Image J). For FL-FAK and FK-FAKwt, autophosphorylation is significantly faster in the presence of PI(4,5)P_2 vesicles, while mutations in the basic patch of FK-FAK-KAKTLRK abrogate this effect. *(C)* Autophosphorylation efficiency of FK-FAK (wt or 180/183A mutant) was assessed using an ELISA method. The presence of C8-PI(4,5)P_2, but not C8-PC or the head group Ins(1,4,5)P_3, enhance autophosphorylation of FK-FAKwt to levels similar to FK-FAK180/183A, which was not affected by PI(4,5)P_2. *(D)* Catalytic steady-state activity was assayed for the indicated FAK proteins using a kinase assay, which couples ADP production to NADH consumption (see methods). Whereas dissociation of FERM/kinase domains by mutation (180/183A) activates FAK, none of the tested lipids increase catalytic turnover. *(C-D)* Error bars represent SD from three experiments.

Many stimuli have been reported to initiate FAK activation (reviewed in(27), such as integrin signaling and engagement of growth factor receptors (28-30), but molecular details remain elusive. Further, we showed that acidic phosphoinositides, such as phosphatidylinsositol-4,5-bisphosphate (PI(4,5)P_2), interact with FAK and play a role in FAK activation (31). PI(4,5)P_2 is well established as a modulator of FA maturation and adhesion strength, but its role in adhesion signaling is less clear. PI(4,5)P_2 promotes formation of mature FAs by binding talin and vinculin and inducing their open state where binding sites to other FA proteins and actin are exposed (32, 33). PI(4,5)P_2 is locally generated in FAs by the enzyme phosphatidylinositol 4-phosphate 5-kinase type Iγ (PIP5KIγ) (34, 35), which adds the 5-phosphate to PI(4)P. PIP5KIγ exists as two splice variants (PIP5KIγ661 and PIP5KIγ635 in mice) where the longer form (PIP5KIγ661; PIP5KIγ668 in human) contains extra C-terminal residues that target the enzyme to FAs by interacting with the talin head domain (36, 37).

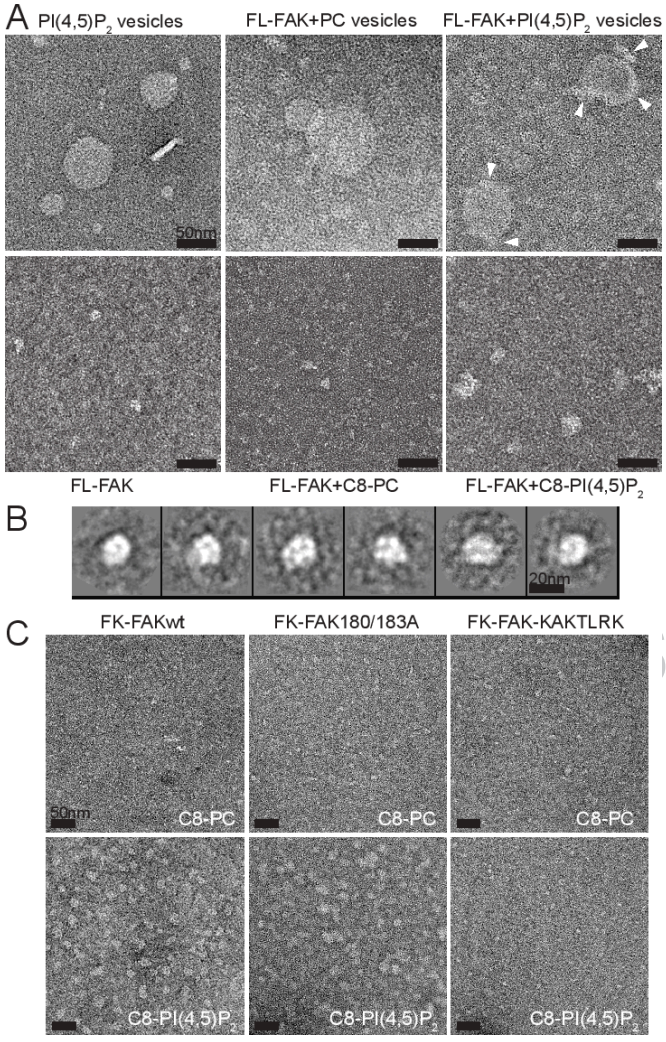

Fig. 3. Electron microscopy reveals PI(4,5)P_2 induced FAK clustering. *(A)* Transmission electron micrographs of FL-FAK with lipid vesicles (upper panels) or soluble lipids (lower panel) imaged by negative staining. PI(4,5)P_2 vesicles and soluble C8-PI(4,5)P_2 mediate the formation of FAK clusters. Clusters on vesicles are indicated by arrowheads. *(B)* Reference free 2D class averages of 574 FL-FAK/C8-PI(4,5)P_2 clusters reveals a homogeneous size of clusters with features that suggest an internal organization. Volume calculations suggest that clusters consist in the range of 6-8 FL-FAK molecules per cluster. *(C)* FK-FAKwt as well as 180/183A and KAKTLRK mutants were imaged in the presence of C8-PI(4,5)P_2 or C8-PC. FK-FAKwt and FK-FAK180/183A, but not the KAKTLRK mutant display clustering in the presence of PI(4,5)P_2. *(A and C)* Scale bars represent 50 nm.

Although the main players involved in FAK activation have been identified, at a mechanistic level it is not known how their concerted action is orchestrated to achieve FAK activation. Here, we probe the molecular mechanism of FAK activation using a multidisciplinary approach, including biochemical, structural, *in vitro* FRET, molecular dynamics (MD) simulations and cell biology studies and we present evidence that PIP5KIγ and its product PI(4,5)P_2 are important mediators of the integrin-FAK signaling link. Intriguingly, we find that PI(4,5)P_2 binding to a basic region on the FAK FERM domain results in clustering of FAK on the lipid membrane, a process likely to enhance integrin clustering as well as the scaffolding function of FAK. PI(4,5)P_2 binding further induces conformational changes between FERM and kinase domains, without causing domain dissociation. *In vitro* FRET experiments together with MD simulations support a scenario where distal changes at the PI(4,5)P_2 binding site result in domain opening and exposure of linker regions, which together with clustering promote efficient autophosphorylation of Y397 within the linker. FAK autophosphorylation recruits Src and in turn Src is responsible for full activation of FAK and FERM release by phosphorylating the FAK activation loop. This new insight in the mechanism of FAK activation will aid the design of novel classes of therapeutics targeting both, catalytic and scaffolding functions of FAK.

RESULTS

FAK specifically binds PI(4,5)P_2 via basic residues in the FERM F2 lobe

In order to characterize the FAK-PI(4,5)P_2 interaction in detail we performed *in vitro* binding studies. Using vesicle pulldown experiments we initially analyzed the phosphoinositide specificity and find that phosphates on the D4 and D5 positions of the inositol ring are the main determinants for binding, whereas the D3 phosphate has no effect (Fig. 1B). This suggests the enzyme PIP5KIγ as a key enzyme regulating FAK signaling. Other phospholipids, such as phosphatidyl inositol (PI), phosphatidyl serine (PS) or phosphatidyl choline (PC) only display background levels of binding. The FERM domain of FAK (F-FAK) is sufficient for full PI(4,5)P_2 binding affinity (Fig. 1C) and binding is mediated via a conserved basic region in the FERM F2 lobe as shown by mutation of the basic KAKTLRK sequence (all K/R to A=FAK-KAKTLRK, Fig. 1A, 1D). Interestingly, the FERM+kinase fragment of FAK (FK-FAK) interacts with approximately 2 fold lower affinity than F-FAK (Fig. 1C, 1D). In addition, a mutant form of FK-FAK where residues Y180 and M183 in the FERM F2 lobe are mutated to alanine (FK-FAK180/183A) displays, like F-FAK, higher PI(4,5)P_2 affinity than FK-FAKwt (Fig. 1A, 1D). This observation is supported by surface plasmon resonance experiments (Fig. S1A). The residues Y180 and M183 are located at the region of the FERM F2 lobe that is responsible for kinase binding and autoinhibition (21) (Fig. 1A). Using small-angle X-ray scattering we show that the 180/183A mutant of FK-FAK adopts an open conformation with FERM and kinase domains dissociated (Fig. S2) in contrast to FK-FAKwt which adopts a closed conformation (21). We therefore conclude that the reduced affinity of closed FK-FAKwt (seen in Fig. 1D and S1) is due to an energetically costly conformational change required to bind PI(4,5)P_2. Further, we find that C-terminal regions of FAK do not affect PI(4,5)P_2 binding, since full-length FAK (FL-FAK) exhibits a similar PI(4,5)P_2 affinity as FK-FAK (Fig. 1E). Importantly, the PI(4,5)P_2 affinity of FAK is altered by the PI(4,5)P_2 density on lipid vesicles, indicating an avidity effect. Doubling the PI(4,5)P_2 concentration from 6 to 12% (mol/mol) increases the affinity approximately 4 fold (Fig. 1E). For simplicity we use a one-site model to fit our pulldown data presented in Fig.1C-E, however the data fits well with a cooperative model indicating positive cooperatively with a hills coefficient of ∼2 (Fig.S1B).

PI(4,5)P_2 enhances FAK autophosphorylation without increasing catalytic turnover

Next we tested the effect of PI(4,5)P_2 on FAK kinase activity. Using an autophosphorylation assay, we find that PI(4,5)P_2 vesicles strongly increase the autophosphorylation efficiency as shown by immuno blotting using an antibody against the autophosphorylation site Y397 (Fig. 2A, 2B), whereas PI(4)P and PI(3,4)P2 have no effect (Fig.S3A). As is the case for PI(4,5)P_2 binding, enhanced autophosphorylation requires the basic KAKTLRK region. Using soluble PI(4,5)P_2 (with 8 carbons in the acyl chain, C8-PI(4,5)P_2), we measured autophosphorylation via an ELISA assay and find that C8-PI(4,5)P_2 increases the autophosphorylation efficiently of FK-FAKwt to similar levels as observed for FK-FAK180/183A (Fig. 2C). Although the PI(4,5)P_2 head group is necessary for this effect (compare C8-PI(4,5)P_2 vs. C8-PC plot in Fig. 2C) the head group alone (Ins(1,4,5)P_3)

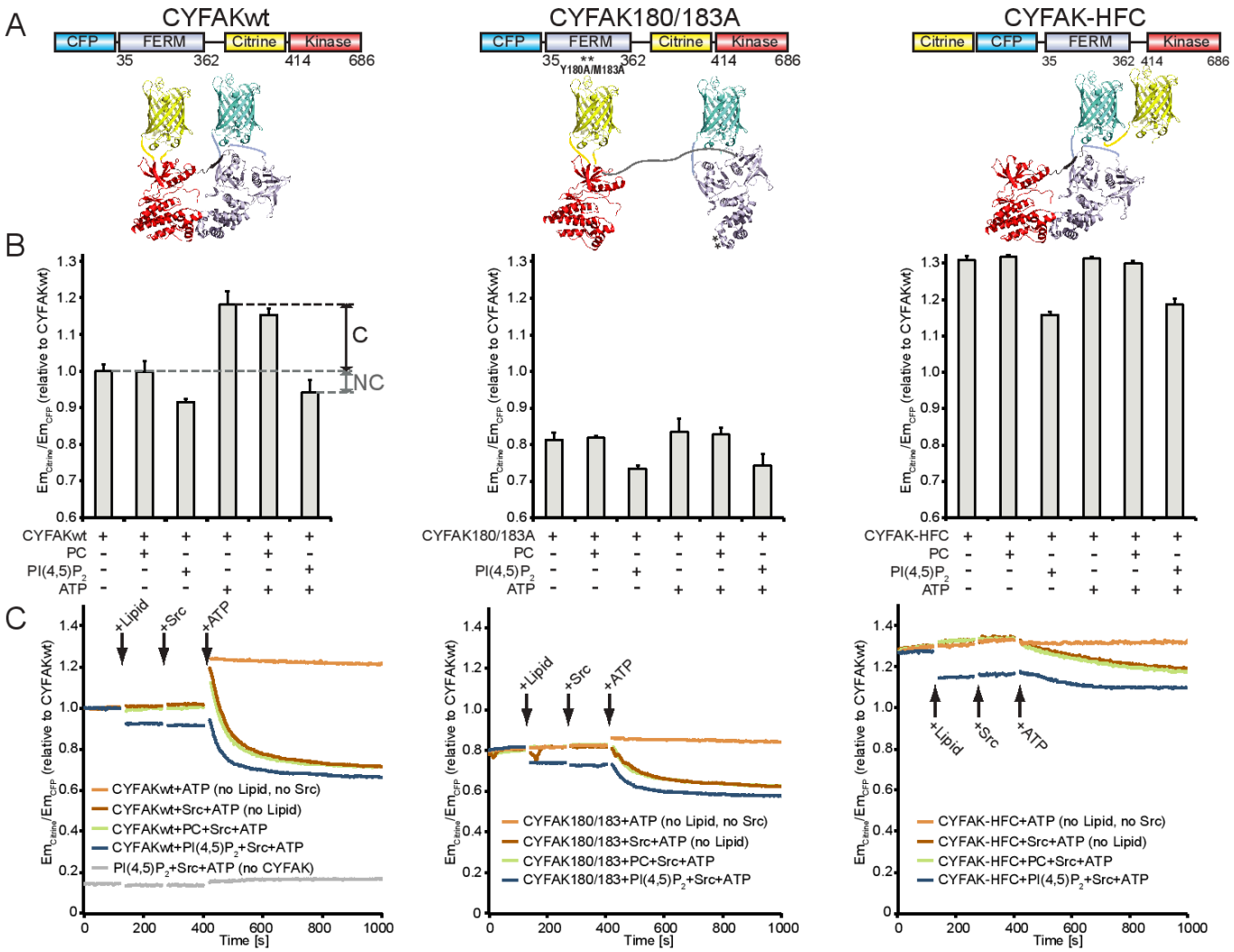

Fig. 4. PI(4,5)P_2 induces partial and Src full domain opening of the FAK FRET sensor in the presence of ATP. *(A)* Schematic illustration of domain structure (top) and expected structural arrangement (bottom) of the conformational FRET sensors used. *(B)* The emission ratios of citrine and CFP are plotted relative to CYFAKwt as a measure of FRET. The presence of C8-PI(4,5)P_2 causes a reduction in FRET levels for all 3 sensors, suggesting that this effect is not conformational (labeled NC). The presence of ATP significantly increases FRET levels for CYFAKwt, but not in the presence of PI(4,5)P_2. The effect of ATP is not seen for CYFHFC and is therefore likely conformational (labeled C). *(C)* Relative FRET levels were monitored in real time, initially of the sensors alone, and then following addition of: i) Lipid: C8-PC (green plots), C8-PI(4,5)P_2 (blue plots) or no lipid (brown and orange plots), ii) Src (brown, green and blue plots) or no Src (orange plots) and iii) ATP/Mg^{2+} (all plots). As in panel (B) PI(4,5)P_2 reduces FRET levels of all sensors in all states (before/after phosphorylation) indicating a non-conformational effect. ATP results in a FRET spike only with CYFAKwt. If active Src is present, the spike is followed by a switch to the open conformation (lower FRET levels). In contrast inactive SrcK298M induces only a modest FRET decrease (see Fig.S5C). The grey control plot in the left panel is without CYFAK sensor to verify that PI(4,5)P_2, Src and ATP do not exhibit intrinsic fluorescence.

is not sufficient. Remarkably, neither soluble nor vesicle embedded PI(4,5)P_2 affect the catalytic activity as measured by ATP turnover in a kinetic assay with an exogenous substrate (Fig. 2D, S3C, S3D). The fact that dissociation of FERM and kinase domains by mutation does increase ATP turnover, as shown with the FK-FAK180/183A mutant (Fig. 2D, S3C, S3D), suggests that PI(4,5)P_2 binding to FAK does not dissociate the FERM from the kinase domain.

PI(4,5)P_2 induces FAK clustering

Since FAK has been shown to efficiently autophosphorylate in *trans* (23), we considered the possibility that PI(4,5)P_2 induced autophosphorylation might be mediated via FAK oligomers. Using negative-stain transmission electron microscopy, we show that FAK forms clusters on PI(4,5)P_2 vesicles as well as bound to soluble C8-PI(4,5)P_2 (Fig. 3A). Reference free 2D class averaging of FL-FAK clusters bound to C8-PI(4,5)P_2 reveals a homogeneous size of clusters (Fig. 3B). Based on 3D volumes generated from 2D averages or particle dimensions, we determined an approximate particle size of 900 kDa, from which we estimate the presence of approximately 6-8 FL-FAK molecules per cluster. Size measurements on single particles (un-averaged) reveal that FL-FAK and FK-FAK clusters exhibit similar dimensions, indicating that C-terminal regions might not contribute to the core of clusters (Fig.S4A). Like PI(4,5)P_2 binding, formation of clusters requires the basic KAKTLRK region on the F2 lobe (Fig. 3C, bottom panels). Using dynamic light scattering we show that PI(4,5)P_2 also induces an increase in molecular weight for F-FAK (Fig. S4B). We confirmed that C8-PI(4,5)P_2 induced clusters do not form as a consequence of micelle formation, since we determined a CMC for C8-PI(4,5)P_2 of 2 mM, an order of magnitude higher than used in our study.

PI(4,5)P_2 prevents formation of a fully closed conformation

As described above, we believe that PI(4,5)P_2 does not induce dissociation of FERM and kinase domains. However, the fact

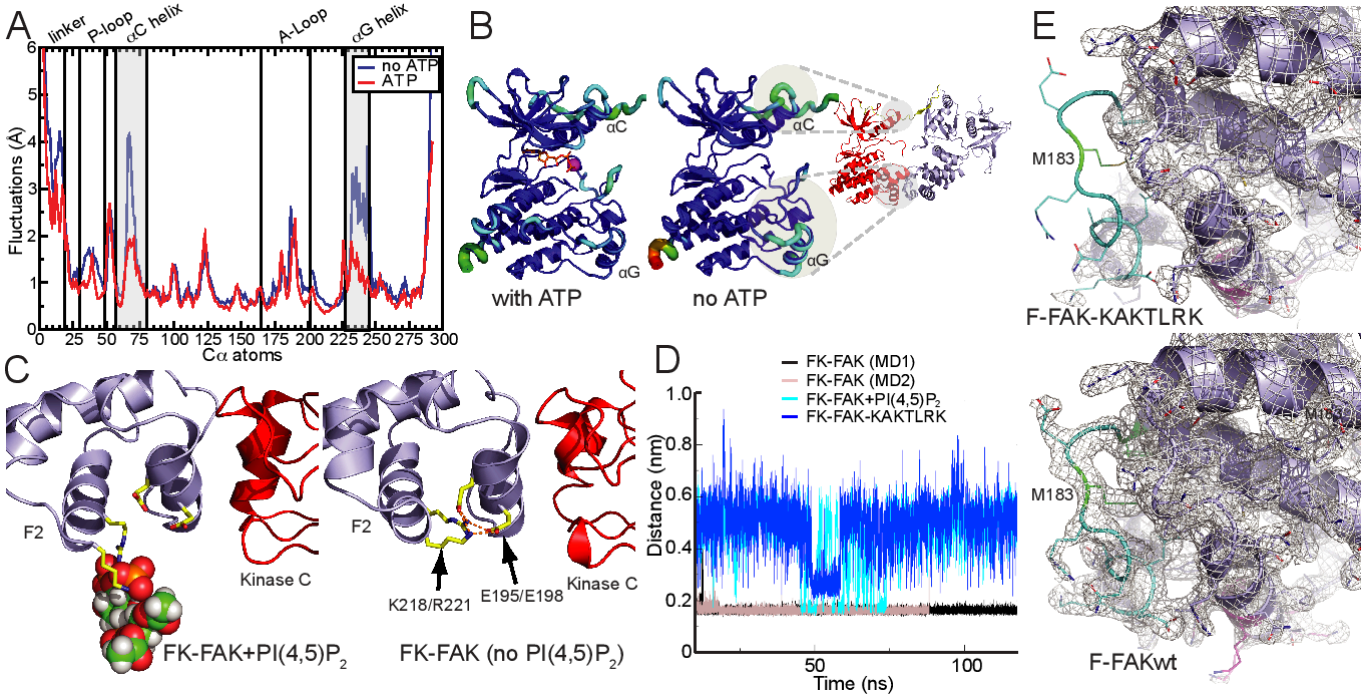

Fig. 5. Effects of ATP and PI(4,5)P_2 on FAK conformation. *(A)* Root mean square fluctuations (RMSFs) from unbiased MD simulations of the FAK kinase are shown for a window of 700 ns (discarding the first 200 ns of equilibration) for the FAK kinase alone (blue plot) and FAK with ATP/Mg^{2+} (red plot). ATP binding stabilizes the αC and αG helices. *(B)* RMSF values from panel (A) are color mapped onto the FAK kinase structure. RMSFs range from blue (low values) to red (high values). Stabilizing ATP effects on αC and αG helices map autoinhibitory interaction sites as seen in the FK-FAK crystal structure (21). *(C)* Neutralization of the basic patch by PI(4,5)P2 binding (or by mutation, see panel D) interferes with a set of FERM F2-lobe stabilizing salt bridges. MD simulations suggest that salt bridges between K218/R221 in the basic patch and E195/E198 are formed in the absence (right), but not in the presence of PI(4,5)P2 (left), leading to a partial destabilization of the FERM F2 lobe and an altered force distribution as shown in Fig.S7a. *(D)* Minimum distances for the residues K218/R221 and residue pair E195/E198 are shown during MD simulations with FK-FAK alone (MD1, MD2), FK-FAK bound to PI(4,5)P_2 or the basic patch mutant FK-FAK-KAKTLRK. In the two independent MD simulations of FK-FAKwt, these two pairs of oppositely charged residues strongly interact with each other. PI(4,5)P_2 binding or KAKTLRK mutations to alanines significantly increases the minimum distances and fluctuations. *(E)* Crystal structure of the basic patch mutant FERM domain (F-FAK-KAKTLRK, for full structure, see Fig. S7C). In contrast to F-FAKwt (bottom), the structure of F-FAK-KAKTLRK (top) exhibits no electron density for the loop (cyan) containing the autoinhibitory residues Y180/M183 (green), indicating that this loop is disordered. 2Fo-Fc electron density maps are shown as grey mesh countered at 1σ.

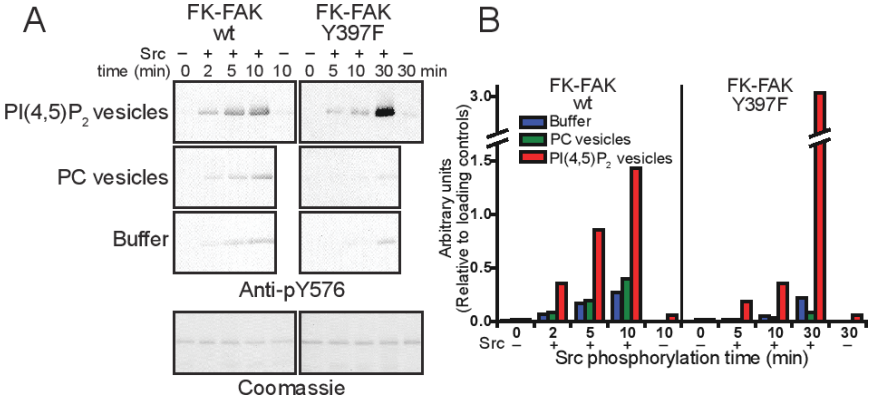

Fig. 6. PI(4,5)P_2 enhances Src phosphorylation of Y576 in FAK. *(A)* A time course of Src phosphorylation of FK-FAK in the absence or presence of PI(4,5)P_2 or PC vesicles as monitored by western blot using an anti-pY576 antibody, following a 2 min autophosphorylation reaction (see methods). Mutation of the autophosphorylation site (Y397F) significantly reduces the Y576 phosphorylation rate, wheras PI(4,5)P_2 enhances Y576 phosphorylation for FK-FAKwt and FK-FAK-Y397F, indicating a combined effect of more efficient Src recruitment to the FAK autophosphorylation site and PI(4,5)P_2 induced conformational changes. Bottom panels are Coomassie stained loading controls. *(B)* The quantifications of blots in (A) are shown.

that the open FK-FAK180/183A mutant exhibits higher affinity for PI(4,5)P_2 than closed FK-FAKwt (Fig. 1D, S1A), suggests that closed FK-FAK requires a rearrangement of FERM and kinase domains to allow PI(4,5)P_2 binding. To monitor conformational changes in a controlled environment we employed *in vitro* FRET experiments using a conformational sensor of FAK. A similar sensor we used previously in cellular studies to demonstrate that FAK undergoes conformational changes in FAs (31). The sensor is based on intramolecular FRET by fusing CFP and citrine N-terminal to the FERM and kinase domains respectively, and is designed to report relative domain positions, with autoinhibited (closed) FAK exhibiting high FRET and open forms displaying lower FRET signals. We used three purified versions of the sensor that contain the FERM and kinase regions of FAK (Fig. 4A): i) a sensor with wild-type FAK sequence (CYFAKwt), ii) a sensor which is mutated to adopt an open conformation (CY-FAK180/183) and iii) a high FRET control sensor (CYFAK-HFC) which has the FRET labels in tandem at the N-terminus and hence displays high FRET signals independent of the intramolecular FAK conformation. Changes in FRET levels of the CYFAK-HFC sensor indicate non-conformational effects, such as trans-FRET or fluorescence quenching (which for example could be

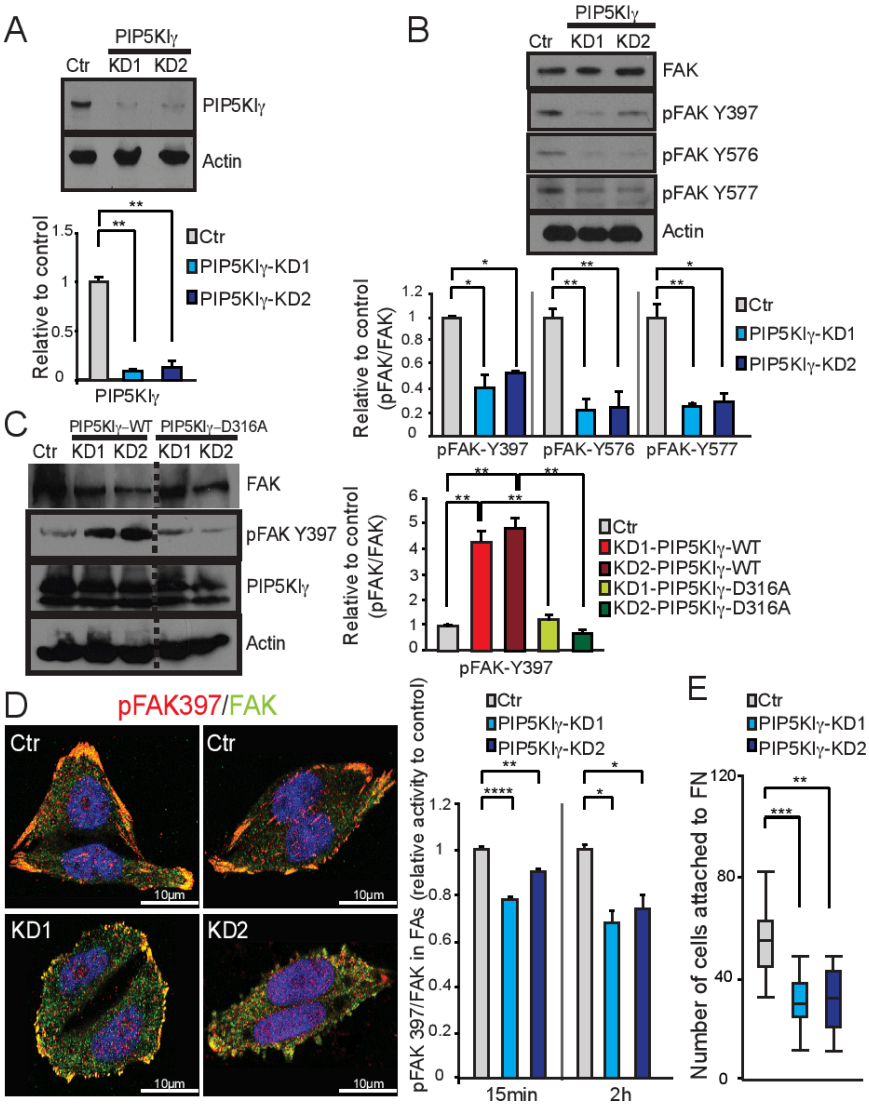

Fig. 7. PIP5KIγ knockdown decrease cellular FAK activity and cell attachment. *(A)* Expression levels of PIP5KIγ668 (isoform 2) in HeLa cells after knockdown are shown for two different clones (KD1 and KD2) and scramble control (Ctr). A representative immunoblot is shown; the quantification of PIP5KIγ levels observed by immunoblot is depicted in the bottom histogram. Quantifications are from 4 blots (2 independent experiments, each in duplicates). *(B)* Effect of PIP5KIγ reductions on the total level of FAK, and on the total cellular levels of pFAK Y397, Y576 and Y577. A representative immunoblot, and the quantification from 4 blots (2 independent experiments, each in duplicates) are shown. *(C)* pFAKY397 levels in HeLa cells of Ctr or KD1 and KD2 cells transfected with WT (PIP5KIγ-WT) or a kinase-dead (PIP5Kγ-D316A) form of PIP5KIγ. Immunoblot and quantifications of two independent experiments are shown, each performed twice. Note that PIP5KIγ-WT more than rescues but the kinase dead mutant does not fully rescue FAK phosphorylation levels in KD cells compared to controls. Dashed lines merge different lanes of the same immunoblot experiment *(D)* Immunofluorescence staining of pFAK397 (red) and total FAK (green) in PIP5KIγ KD1 and KD2 clones and scramble controls (Ctr), and the quantification of the immunofluorescence intensity of pFAK397 relative to total FAK signals specifically in FAs at 15 min and 2h after stimulation with serum and fibronectin is shown. *(E)* Functional cell adhesion assay to determine the ability of PIP5KIγ deficient cells to attach to fibronectin compared to scramble controls. Quantification of the number of attached cells for 3 independent experiments in triplicates is shown. Data represent the mean value ± s.e.m.; *p<0.05, **p<0.01, ***p<0.001, ****p<0.0001, unpaired Student's t-test.

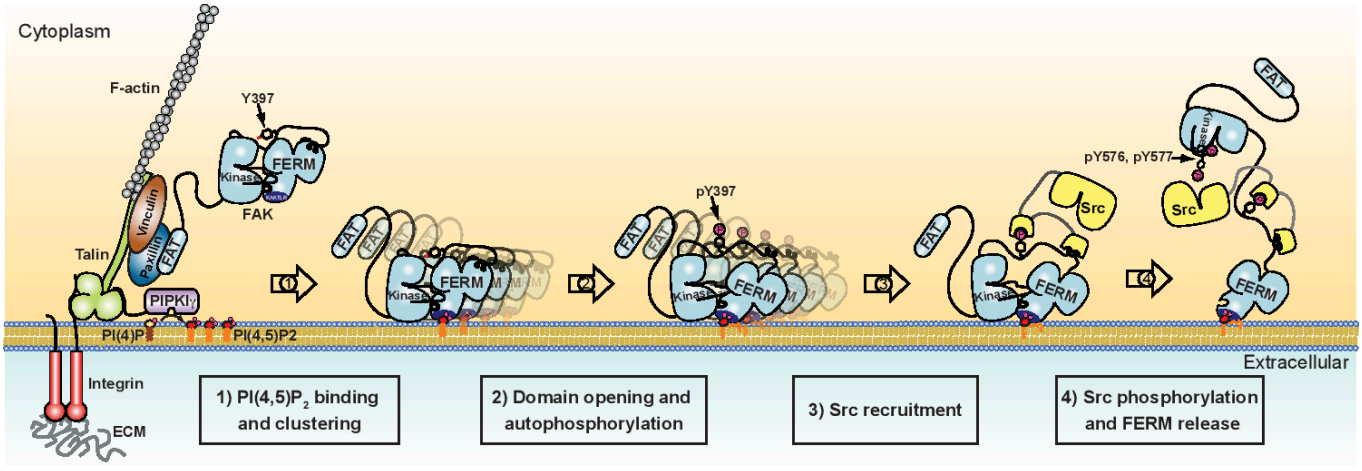

Fig. 8. Schematic model for integrin mediated FAK activation by PI(4,5)P_2. Cell adhesion via integrin receptors to the extracellular matrix (ECM) results in integrin clustering and the recruitment of FA proteins (as here illustrated for talin, vinculin, paxillin, FAK and PIP5KIγ) to form adhesion structures that link integrins to the actin cytoskeleton (left). Recruitment of PIP5KIγ results in local increase of PI(4,5)P_2 levels in FAs. PI(4,5)P_2 in FAs binds FAK via the basic patch (dark blue) in the FERM domain of FAK resulting in FAK clustering at the cell membrane (step 1). PI(4,5)P_2 induced FAK clustering results in a relaxed FERM/kinase conformation, with the kinase N-lobe dissociated from the linker and FERM F1 lobe. PI(4,5)P_2 induced clustering and conformational relaxation allows efficient autophosphorylation of Y397 (step 2) and Src recruitment via SH2 and SH3 domains (step 3). Recruited Src phosphorylates the activation loop residues Y576/Y577 of FAK, which results in full activation and release of the kinase from the membrane clustered FERM domain (step 4).

caused by clustering). As expected we find lower FRET levels for the open CYFAK180/183A sensor than for CYFAKwt and high FRET levels for CYFAK-HFC (Fig. 4B, left bars in each panel, Fig. S5A). The addition of C8-PC does not affect FRET levels, however, C8-PI(4,5)P_2 induces a reduction in FRET signals for all 3 sensors (Fig. 4B, 4C). Since PI(4,5)P_2 also affects CYF-HFC, which reports non-conformational effects, we conclude that under these conditions (without ATP, see below) PI(4,5)P_2 does not significantly alter the conformation of FAK.

Interestingly, when we added ATP and Mg^{2+} to CYFAKwt the FRET signal increased almost to the level of CYF-HFC (Fig. 4B, 4C). This effect is not seen with CYFAK-HFC and is therefore likely conformational, with higher FRET signals suggesting a more closed conformation in the presence of ATP. This increase in FRET is not due to a phosphorylation event since the same effect is seen with the non-hydrolysable ATP analogue AMP-PNP (Fig. S5B). Importantly, the high-FRET state with ATP is not observed in the presence of PI(4,5)P_2 (Fig. 4B, 4C, left panels) and in fact is reverted in a concentration dependent manner by PI(4,5)P_2 if added after ATP (Fig.S5D). This indicates a conformational effect of PI(4,5)P_2 in the presence of ATP. Since ATP is present in the cell at similar concentrations we used in our experiments (1mM), the high-FRET state observed in presence of ATP likely represents the basal conformation of FAK which is affected by PI(4,5)P_2. When comparing FRET levels of CYFAKwt in the presence of ATP with and without PI(4,5)P_2 we can partition the FRET change into a non-conformational effect of PI(4,5)P_2, which is also seen without ATP (NC in Fig. 4B), and a larger conformational effect (C in Fig. 4B). When the PI(4.5)P2 induced reduction in FRET is corrected for the non-conformational part, FRET levels of CYFAKwt in presence of ATP approach levels without ATP. (Fig.S5D right panel). The FRET change even at high PI(4,5)P2 concentrations does, however, not correspond to full domain dissociation (see below). Together this data suggest that in the presence of ATP, PI(4,5)P_2 induces partial domain opening.

In experiments where Src is present in addition to CYFAKwt and ATP, the initial increase in FRET is followed by a switch to an open conformation (lower FRET signals, Fig. 4C left panel), whereas only a minor effect is observed for the CYFAK-HFC control. The kinase dead mutant SrcK298M has a small effect on FRET levels in presence of ATP (Fig.S5C), therefore we conclude that Src phosphorylation is mainly responsible for switching CY-FAKwt to the open conformation, and Src binding has a minor effect. This is consistent with observations that Src phosphorylation of the FAK activation loop is incompatible with FERM inhibition (21). Comparing FRET signals of different states corroborates that PI(4,5)P_2 does not induce a full FERM/kinase dissociation, which is observed only upon Src phosphorylation or 180/183A mutation. Since domain association is mainly determined by the FERM F2/kinase C-lobe interaction (21) (Fig. S2), we propose that the partial opening induced by PI(4,5)P_2 occurs likely at the FERM F1/linker/kinase N-lobe site.

Allosteric effects of PI(4,5)P_2 on the FERM/kinase interface

Since the two opposite effects of PI(4,5)P_2 and ATP appear to be related, we first proceeded to better understand the effect of ATP. Using MD simulations we monitored backbone fluctuations of the solvated FAK kinase domain in presence or absence of ATP over 1500 ns. We find that the presence of ATP in the active site has the largest stabilizing effect in the αC and αG helices of the FAK kinase domain (Fig. 5A). Strikingly, these two sites exactly map the autoinhibitory interaction sites with the FERM domain as seen in the crystal structure of FK-FAK (21) (Fig. 5B). In accordance with FRET and simulation data, we therefore propose that binding of ATP to the FAK kinase induces a tightly closed FERM-kinase conformation by rigidifying the interaction interfaces. Moreover, by performing an elastic network-based allosteric connectivity analysis of the FAK kinase domain we find by a completely independent computational approach (38) a strong allosteric coupling between αC and αG helices despite their distal locations (Fig. S6).

We then proceeded to probe conformational effects of PI(4,5)P_2 by performing MD simulations of (i) FK-FAK alone, (ii) bound to soluble PI(4,5)P_2 (C2-PI(4,5)P_2) or iii) with the basic patch mutant FK-FAK-KAKTLRK. Interestingly, we find that PI(4,5)P_2 binding results in altered inter-residue forces within the FERM F2 lobe that originate at the basic patch and propagate to the interface with the kinase C-lobe (Fig. S7A top). In particular, PI(4,5)P_2 binding interferes with a set of stabilizing salt bridges between the basic patch (K218/R221) and the adjacent helix at the domain interface (E195/E198, Fig. 5C, 5D). These PI(4,5)P_2-induced changes also affect the loop containing the autoinhibitory residues Y180 and M183. This effect was reproduced in MD simulations of FK-FAK-KAKTLRK (Fig. 5D, S7A bottom, S7B), suggesting that neutralizing the charges of the basic KAKTLRK residues by mutation has a similar effect on the FERM F2-lobe interatomic forces as PI(4,5)P_2 binding. We validated our model for the PI(4,5)P_2-FERM-F2 lobe interaction by performing MD simulations with PI(4,5)P_2 embedded in a lipid bilayer and find that the mode of the FERM-PI(4,5)P_2 interaction is highly similar. PI(4,5)P_2 remains embedded in the bilayer (at least within the time scale of the simulations) such that the PI(4,5)P_2-FAK interaction is restricted to the head group, therefore like with short-chain lipids, MD simulations primarily provide details on a charge neutralization effect.

In the absence of a FAK-PI(4,5)P_2 co-crystal structure, which is complicated by clustering as seen in Fig. 3 and S4, we pursued a crystal structure of the basic patch mutant FERM domain (F-FAK-KAKTLRK, crystallographic table S1). Although overall the FERM domain retains a very similar conformation to F-FAKwt, in both independent molecules in the asymmetric unit cell, no electron density is observed for the loop Y180-K190 (containing the autoinhibitory residues Y180/M183), indicating that the loop is disordered (Fig. 5E, S7C). This is in striking agreement with observations from MD simulations described above, which find a destabilized F2 lobe upon neutralization of the basic region in the FERM F2 lobe (Fig. 5C-D, S7A-B). In conclusion, we propose that neutralization of the basic patch by specific binding of PI(4,5)P_2 destabilizes the FERM F2 lobe resulting in an altered FERM F2/kinase C-lobe interface, which allows domain opening.

PI(4,5)P_2 enhances Src mediated FAK activation

FAK activation proceeds through a multistep mechanism. PI(4,5)P_2 induced FAK autophosphorylation is followed by Src recruitment to the autophosphorylation site and phosphorylation of the activation loop of FAK (residues Y576, Y577) by Src. Since Src recruitment requires FAK autophosphorylation, it can be expected that PI(4,5)P_2 should also enhance Src mediated phosphorylation of the activation loop of FAK. To test this, we monitored Src phosphorylation of Y576 in the presence or absence of PI(4,5)P_2 by immuno blotting, using an antibody against phospho-Y576, following an autophosphorylation step (Fig. 6). In order to uncouple auto- from Src phosphorylation, autophosphorylation was stopped after 2 min with the specific FAK inhibitor TAE226 before starting Src reactions (see methods for details). As expected, we find that Y576 phosphorylation is more efficient in the presence of PI(4,5)P_2, whereas other tested phosphoinositides have no effect (Fig.S3B). To a large part this effect is due to enhanced FAK autophosphorylation, since in the absence of autophosphorylation (for FK-FAK Y397F) Y576 phosphorylation by Src is greatly reduced at equivalent time points (note that in Fig.6 we added a longer 30 min time point for FK-FAK Y397F due to weak phosphorylation levels at 10 min). However, PI(4,5)P_2 also enhances Src phosphorylation of the FK-FAK Y397F mutant, suggesting also an autophosphorylation independent effect. This

data is consistent with $PI(4,5)P_2$ inducing an open conformation which allows easier access to Y576.

$PI(4,5)P_2$ in FAs promotes FAK signaling and cell adhesion

We have previously proposed acidic phospholipids to be involved in FAK activation in cells (31), however, the lipid specificity and hence relevant upstream components were not defined. Since we show $PI(4,5)P_2$ specificity (Fig.1B) and PIP5KIγ is known to be responsible for $PI(4,5)P_2$ generation in FAs, we performed PIP5KIγ loss of function experiments in HeLa cells to establish the role of $PI(4,5)P_2$ in FAK signaling in FAs. The expression of PIP5KIγ was knocked-down using a specific shRNA against the isoform 2 of PIP5KIγ (the longer PIP5KIγ668 isoform), and two different stable knockdown clones were selected (KD1 and KD2). The knockdown efficiency was very high, as observed by Western Blotting and immunofluorescence (Fig. 7A, S8A). The total levels of FAK did not change in the absence of PIP5KIγ (Fig. 7B). However, the status of the Y397 autophosphorylation site, and Y576, Y577 Src phosphorylation sites was significantly reduced at early stages of focal adhesion formation, when compared to the scramble controls (Fig. 7B). Overall, these data suggest that PIP5KIγ may function in the proper activation of FAK. To validate the causal role of PIP5KIγ in the activation of FAK, we performed rescue experiments, using vectors encoding either a WT (PIP5KIγ-WT) or a kinase-dead (PIP5Kγ-D316A) form of PIP5KIγ. As shown in Fig. 7C, on a PIP5Kγ deficient background, expression of PIP5KIγ-WT not only restored but increased the phosphorylation levels of pFAKY397 when compared to the scramble controls. By contrast, the expression of the PIP5Kγ-D316A kinase dead mutant in PIP5Kγ deficient cells was not able to fully rescue pFAKY397 levels (Fig. 7C). Overall, these data provide evidence that PIP5Kγ kinase activity is required for the activation of FAK at least in some cellular contexts.

Immunofluorescence analysis revealed that the effect of PIP5Kγ knockdown on the activation of FAK was not due to an impairment of the recruitment of FAK to FAs. FAK was recruited to FAs in KD cells from early time points of stimulation, although the pFAKY397 levels were reduced when compared to controls (Fig. 7D, S8B). Interestingly, KD cells displayed smaller FAs (Fig. S8C). To analyze the functional relevance of PIP5Kγ in FAs, we further evaluated the ability of PIP5Kγ-deficient cells to attach to fibronectin-coated plates at early stages of cell adhesion and spreading. In comparison to controls, fewer PIP5Kγ-deficient cells attached to the plates (Fig. 7E), indicating that PIP5Kγ is required to promote the adequate adhesive properties of FAs. Globally, these data establish PIP5KIγ and its product $PI(4,5)P_2$ as upstream activators of FAK in FAs and suggest they play important roles in FA maturation, cell attachment and spreading.

DISCUSSION

All non-receptor tyrosine kinases (NRTKs) utilize remarkably similar concepts to switch kinase activity off. In all known cases, regulatory domains N-terminal to the tyrosine kinase domain bind the kinase to induce autoinhibition and in many cases this sequesters regulatory phosphorylation sites. Also initial activation steps often follow similar principles. For Src, Abl and Syk family tyrosine kinases, activation is initiated by activator binding to their regulatory domains, which induces release of the regulatory domain from the kinase resulting in activation. In the case of FAK, autoinhibition is achieved as for other NRTKs, by the regulatory FERM domain docking onto the kinase domain (21). It was widely assumed that also activation would follow the canonical path of ligand induced release of the FERM domain. This was partially based on studies showing that FAK undergoes large conformational changes in FAs (31). Here we show that with respect to the activating $PI(4,5)P_2$ ligand the situation is different for FAK. FAK is in many ways an outsider among NRTKs, in that it is localized to a highly dense and clustered environment (FAs) where it has been proposed not only to act as an active kinase but also as a scaffolding protein. Our data indicate that $PI(4,5)P_2$ induced activation of FAK follows concepts distinct from other NRTKs that are adapted to a highly crowded environment and allow concerted scaffolding and catalytic function.

Our findings support a rather complex model of sequential FAK activation presented in Fig. 8. Firstly, we establish $PI(4,5)P_2$, generated in FAs by PIP5KIγ, as an important signaling messenger upstream of FAK activation. We had previously shown that acidic phospholipids, including $PI(4,5)P_2$, bind FAK (31), however, the phospholipid specificity was not established. Here we show that addition of the 5-phosphate in $PI(4,5)P_2$ confers full binding affinity (Fig. 1B) and that PIP5KIγ is an upstream activator of FAK in HeLa cells (Fig. 7). It has been a long-standing question in the field how integrin signaling links to FAK activation. Since integrin signaling specifically results in PIP5KIγ recruitment and local $PI(4,5)P_2$ production (34, 35), we propose that the path of the integrin-FAK signaling link leads via PIP5KIγ and generation of $PI(4,5)P_2$ (Fig. 8, left). However, FAK signaling is highly complex and the exact upstream signaling events likely vary in different tissue contexts. In platelets, for example, FAK signaling does not depend on PIPKIγ (39). We note that $PI(4,5)P_2$ in general is not as tightly regulated as for example $PI(3,4,5)P_3$ levels, however, the property of the FAK-$PI(4,5)P_2$ interaction appears well suited to the characteristics of $PI(4,5)P_2$ levels in the cell and its localized generation. The avidity effect we observe with increased $PI(4,5)P_2$ density (Fig. 1E) will prevent responding to basal $PI(4,5)P_2$ levels (average estimates in the cell are 1% of total lipid), but allows a sharp and specific response to highly localized $PI(4,5)P_2$ production in FAs by PIP5KIγ. On the other hand, Legate et al. (34) propose that bulk $PI(4,5)P_2$ can partially substitute for local $PI(4,5)P_2$ production, which may explain differential effects of PIP5KIγ depletion in different cell types (39). We note that lipid involvement in FAK activation fits well with super resolution optical microscopy studies showing that FAK in FAs resides in close proximity to the cell membrane (40).

We make the novel observation that $PI(4,5)P_2$ induces FAK clustering (Fig. 3, S4, 8 step1). Together with findings showing FAK autophosphorylation to occur in *trans* (23), this suggests FAK colocalization as an important mechanism promoting FAK trans-autophosphorylation, similar to what is proposed for receptor tyrosine kinases (41). Further, since FAK oligomers are multivalent $PI(4,5)P_2$ binders, clustering likely explains the avidity effect we observe (Fig. 1E), although we can not rule out multiple PI(4,5)P2 binding sites on a single FAK molecule. Clustering together with observed conformational changes raises the possibility that PI(4,5)P2 binding occurs in a cooperative mode. Indeed, our vesicle pulldown data fits well with a cooperative model, indicating positive cooperativity with a Hills coefficient close to 2 (Fig.S1B). FAK clusters with soluble $PI(4,5)P_2$ appear globular in shape (Fig. 3B) and we note that 2D averaged images suggest that FAK molecules are circularly arranged with less density at the center and an opening at one side of the circle. The size of FAK clusters on lipid vesicles appears more extended. Possibly, in the case of FAK clustering on a 2D membrane, the circular FAK arrangement seen with soluble $PI(4,5)P_2$ is opened, allowing further propagation of FAK clusters along the membrane. It is currently unclear how FAK clustering is mediated, but since we observe clustering with soluble $PI(4,5)P_2$ below its CMC concentration, direct protein-protein interactions between FAK molecules are likely involved. A potential site is the conserved W266 and a neighboring pocket involving L327, which are involved in lattice contacts in almost all FAK crystals containing the FERM domain. However, understanding details on clustering interfaces will require extensive future structural analysis of FAK clusters.

As suggested from the multiple binding partners of FAK, the clustering also underlines the importance of the scaffolding function of FAK and suggests that FAK may play an important role in FA architecture. Consistent with this notion we observe that PIP5KIγ knockdown results in smaller FAs (Fig. S8C) and weaker cell adhesion (Fig. 7E), although this effect is not necessarily FAK related, since PI(4,5)P2 affects several other focal adhesion proteins, such as talin. A role of FAK in FA maturation and adhesion strength would seem to contradict early studies that implicated FAK in FA turnover (8, 10). However, it is becoming clear that adhesion dynamics is highly complex and more recent studies find an important role for FAK in increasing adhesion strength (42), particularly in response to rigid substrates and increased tension forces (13).

As mentioned earlier, we are suggesting that in FAK clusters the FERM and kinase domains are not dissociated and therefore the FERM F2/kinase C lobe interface is intact. We base this on the facts that, firstly, $PI(4,5)P_2$ does not increase ATP turnover (Fig. 2D, S3C, S3D), and secondly, the FRET level of CYFAKwt in the presence of $PI(4,5)P_2$ does not decrease to the level of CYFAK in the open conformation (Fig. 4C, S5D). This raises the question how autophosphorylation can occur efficiently in a state where steady-state kinetics is inhibited. As described by Grant and Adams, in kinase-substrate complexes and in scenarios where the enzyme/substrate ratio is close to 1 - both are the case here – phosphorylation rates are not determined by steady-state kinetics, but rather by pre-steady-state kinetics (43); reviewed in (44). In such conditions, each enzyme only has to phosphorylate one substrate and can then stay attached to the substrate (off-rate is irrelevant). Accordingly, we propose that in $PI(4,5)P_2$ induced clusters, FAK molecules arrange in ideal position to phosphorylate their neighboring FAK molecule on the linker Y397 site.

In the closed conformation observed in the FK-FAK crystal structure (21) it does, however, appear unlikely that autophosphorylation would occur efficiently, in particular with the Y397 autophosphorylation site in the linker sandwiched between the FERM-F1 and the kinase N-lobe. In fact, our FRET data suggest that FAK in $PI(4,5)P_2$ clusters does not adopt a fully closed conformation (Fig. 4B, S5D). Although we only have circumstantial evidence, we propose that $PI(4,5)P_2$ induced domain opening occurs at the FERM F1/linker/kinase N-lobe linkage. We base this on: i) $PI(4,5)P_2$ does induce domain opening (Fig. 4, S5D), ii) $PI(4,5)P_2$ does not induce FERM/kinase dissociation (Fig.2D, S3D, 4B-C, S5D) and domain association is controlled by the FERM F2/kinase C-lobe interface (Fig.S2, (21)). Any opening at the FERM F1/linker/kinase N-lobe site will expose the linker for efficient autophosphorylation (Fig. 8, step 2). A recent study by Ritt et al. (45) finds that modifying the linker length greatly affects Y397 autophosphorylation without having a large effect on catalytic activity. This illustrates that, similar to what we find for $PI(4,5)P_2$, autophosphorylation and catalytic activity can be decoupled, and that linker conformation has an important effect on autophosphorylation efficiency. An intriguing question is how binding of $PI(4,5)P_2$ to the distal basic patch on the FERM F2 lobe could affect the FERM F1/linker/kinase N-lobe interface. Our studies support a scenario where neutralization of the KAKTLRK region by $PI(4,5)P_2$ binding results in partial destabilization of the FERM F2 lobe (Fig. 5C-E, S7), allowing higher mobility at the FERM F2/kinase C-lobe interface, which through increased domain movement or the allosteric coupling we observe (Fig. S6) affects the kinase N-lobe linkage to the linker and FERM F1 lobe. We note that, since neither KAKTLRK mutation nor head group binding alone induce enhanced autophosphorylation (Fig.2A-C), it appears that, although necessary, charge neutralization is not sufficient and likely other parts of the lipid, such as triglyceride parts or acyl chains, are involved in clustering and/or promoting conformational changes. Therefore, our MD simulations with mainly charge based $PI(4,5)P_2$ interactions appear not to capture the full effect of $PI(4,5)P_2$, but rather an initial charge neutralization of $PI(4,5)P_2$ phosphates binding to the basic KAKTLRK residues. We do currently not understand how other parts of the $PI(4,5)P_2$ lipid are involved in FAK conformational changes and clustering.

Once FAK is autophosphorylated, Src is recruited via its SH2 and SH3 domains (Fig. 8, step 3). Our data presented in Fig. 6 show that $PI(4,5)P_2$, in addition to mediating FAK autophosphorylation, also enhances Src phosphorylation of Y576 in the activation loop of FAK. Our data indicates that this is achieved by a combined effect of increased recruitment through autophosphorylation and easier access to Y576 due to conformational changes. Using our FRET sensor, we show that Src mediated phosphorylation of the FAK activation loop results in full dissociation of the FERM domain (Fig. 4C, Fig. 8, step 4), fully consistent with the observed structural incompatibility of FERM inhibition and Y576 phosphorylation (21). Therefore, $PI(4,5)P_2$, via promoting auto- and Src-phosphorylation, can trigger full FAK activation. However, clearly additional FAK activators are likely to be important, perhaps depending on the cellular setting. Cytoplasmic portions of several growth factor receptors have been reported to activate FAK (28-30) and for some of them direct mechanisms have been proposed that involve the KAKTLRK region of FAK (28, 29). Phosphorylated tails of the c-Met receptor are reported to interact with the KAKTLRK region resulting in phosphorylation of Y194 in FAK (46). Intriguingly, Y194 is completely buried within the FERM F2 lobe, indicating that perhaps phospho-Met tail interactions could induce similar destabilization of the FERM F2 lobe as we describe for $PI(4,5)P_2$ (Fig. 5C-E, S7), hence exposing Y194 for phosphorylation. However, details of growth factor mediated FAK activation remain to be determined, in particular whether they also involve $PI(4,5)P_2$. Interestingly, EGF stimulated cell migration was reported to depend on PIP5KIγ, indicating an important role for $PI(4,5)P_2$ generation in the case of EGFR signaling (47). On the other hand, using similar FRET sensors to the ones in our study, Ritt et al. (45) demonstrate that FAK can be conformationally activated by increased pH, which could be a route for cancer cells to activate FAK ligand independent. Yet another signal involved in FAK activation could be tension forces generated by actomyosin contraction, since FAK was described as a force sensor (12, 13). The different routes resulting in FAK activation might be active depending on the cellular context. The mechanism we propose is likely restricted to situations where basal $PI(4,5)P_2$ concentrations are limiting FAK signaling and activation can therefore be triggered by local $PI(4,5)P_2$ production.

In conclusion, the combination of our experimental approach with computational simulations has allowed us to propose a complex and detailed multistep activation mechanism for FAK. We propose that $PI(4,5)P_2$ activates FAK via a combination of clustering and conformational changes which promote efficient autophosphorylation, Src recruitment, and in turn full activation by Src phosphorylation. Our findings fit well with observations from numerous cell biology studies that have described FAK signaling at the cell membrane in a highly crowded environment with dual catalytic and scaffolding functions. Our insights into the allosteric regulation and intramolecular communication of FAK could have major implications for the development of new classes of allosteric cancer therapeutics targeting FAK regulatory mechanisms that affect both, catalytic and scaffolding functions of FAK.

Methods

For methods on structure solution, MD simulations, docking of $P(4,5)P_2$, cell biology and more details of methods below, see supplementary information.

Vesicle pulldowns

Lipid vesicles were prepared by mixing dissolved phospholipids (Avanti Polar Lipids) to obtain 6% (mol/mol) phosphoinositide in PC (or as indicated).

Solvent was removed on a rotary evaporator, lipid films were hydrated with 20mM HEPES pH7.5, 150mM NaCl and 1mM TCEP and sonicated until resuspended. Vesicle pulldowns were performed with 2 μM FAK proteins and a serial dilution of vesicles. After 2 hours incubation, vesicles were centrifuged for 30 min at 16,100 x g at 4°C. Supernatants were collected and pelleted vesicles washed and resuspended. Protein in pellet and supernatant were quantified by Bradford method (Biorad).

Kinase activity assays

Autophosphorylation reaction mixtures were split in 3 equal volumes after taking the t=0 sample and buffer (Hepes buffered saline, pH7.5), PC or PI(4,5)P2 vesicles (20 μM on outer leaflet) was added, incubated for 20 min and reactions started by addition of ATP/MgCl. Autophosphorylation was monitored by western blotting using an anti-pY397 antibody and colorimetric staining with 4CN. Alternatively, autophosphorylation levels were measured by ELISA using a PY20 antibody conjugated with HRP and development with TMB. An enzyme-coupled assay using poly(E_4Y) as substrate was employed to determine ATP turnover as described in (21). Plotted in Fig. 2D are negative slopes of NADH depletion. Lipid concentrations are at 100 μM C8-lipids or 1.5 mM lipid vesicles (only PC or 6% (mol/mol) PI(4,5)P_2, equaling 45 μM PI(4,5)P_2 per leaflet). Src phosphorylation of Y576 was monitored by western blot. To prevent confounding results due to low levels of Y576 autophosphorylation, auto- and Src-phosphorylation reactions were performed in 2 separate steps. Initially FAK was allowed to autophosphorylate for 2 min. Autophosphorylation was stopped with the specific FAK inhibitor TAE226 and Src phosphorylation started by adding Src. Blots were developed using an anti-pY576 antibody and colorimetric staining with 4CN.

Electron microscopy

Proteins were prepared in presence of 200 μM C8-PC, C8-PI(4,5)P_2 or polymerized PC liposomes containing 0% or 5% PI(4,5)P_2 PolyPIPosomes. Samples were negatively stained on carbon-coated grids with UrAc and imaged using a Tecnai G2 Spirit electron microscope operated at 120 kV and a Slow Scan CCD or TemCam-F416 4k_4k pixel camera.

FRET measurements

FRET measurements were performed using a CFP excitation wavelength of 410nm and recording emissions at 475nm (CFP) and 525nm (Citrine) and relative FRET levels were obtained by the 525nm/475nm emission ratio.

ACKNOWLEDGMENTS.

We thank staff at the ESRF beamline ID14-4 and Liang Guo at APS beamline 18ID for assistance. Further we thank Diego Megias, head of the confocal Microscopy Unit at CNIO, for his help with FA quantifications. The research was supported by the Spanish MICINN (now MINECO) grants BFU2010-15923 (D.L.) and BFU2009-11885 (M.P-M), the Comunidad Autónoma de Madrid grant S2010/BMD-2457 (D.L.), the BMBF grant Systec (F.G.) and the Klaus Tschira Foundation (F.G.). D.L. is also recipient of a Ramón y Cajal award (RYC-2010-06948).

1. Schiller HB & Fassler R (2013) Mechanosensitivity and compositional dynamics of cell-matrix adhesions. *EMBO Rep* 14(6):509-519.
2. Schaller MD (2010) Cellular functions of FAK kinases: insight into molecular mechanisms and novel functions. *J Cell Sci* 123(Pt 7):1007-1013.
3. Zhao X & Guan JL (2011) Focal adhesion kinase and its signaling pathways in cell migration and angiogenesis. *Adv Drug Deliv Rev* 63(8):610-615.
4. Zamir E & Geiger B (2001) Molecular complexity and dynamics of cell-matrix adhesions. *J Cell Sci* 114(Pt 20):3583-3590.
5. Ashton GH, *et al.* (2010) Focal adhesion kinase is required for intestinal regeneration and tumorigenesis downstream of Wnt/c-Myc signaling. *Dev Cell* 19(2):259-269.
6. Lim ST, *et al.* (2010) Knock-in mutation reveals an essential role for focal adhesion kinase activity in blood vessel morphogenesis and cell motility-polarity but not cell proliferation. *J Biol Chem* 285(28):21526-21536.
7. Peng X, *et al.* (2008) Cardiac developmental defects and eccentric right ventricular hypertrophy in cardiomyocyte focal adhesion kinase (FAK) conditional knockout mice. *Proc Natl Acad Sci U S A* 105(18):6638-6643.
8. Ilic D, *et al.* (1995) Reduced cell motility and enhanced focal adhesion contact formation in cells from FAK-deficient mice. *Nature* 377(6549):539-544.
9. Chen BH, Tzen JT, Bresnick AR, & Chen HC (2002) Roles of Rho-associated kinase and myosin light chain kinase in morphological and migratory defects of focal adhesion kinase-null cells. *J Biol Chem* 277(37):33857-33863.
10. Ren XD, *et al.* (2000) Focal adhesion kinase suppresses Rho activity to promote focal adhesion turnover. *J Cell Sci* 113 (Pt 20):3673-3678.
11. Tomar A & Schlaepfer DD (2009) Focal adhesion kinase: switching between GAPs and GEFs in the regulation of cell motility. *Curr Opin Cell Biol* 21(5):676-683.
12. Tilghman RW & Parsons JT (2008) Focal adhesion kinase as a regulator of cell tension in the progression of cancer. *Semin Cancer Biol* 18(1):45-52.
13. Wang HB, Dembo M, Hanks SK, & Wang Y (2001) Focal adhesion kinase is involved in mechanosensing during fibroblast migration. *Proc Natl Acad Sci U S A* 98(20):11295-11300.
14. Zhao J & Guan JL (2009) Signal transduction by focal adhesion kinase in cancer. *Cancer Metastasis Rev* 28(1-2):35-49.
15. Parsons JT, Slack-Davis J, Tilghman R, & Roberts WG (2008) Focal adhesion kinase: targeting adhesion signaling pathways for therapeutic intervention. *Clin Cancer Res* 14(3):627-632.
16. Schultze A & Fiedler W (2010) Therapeutic potential and limitations of new FAK inhibitors in the treatment of cancer. *Expert Opin Investig Drugs* 19(6):777-788.
17. Arold ST, Hoellerer MK, & Noble ME (2002) The structural basis of localization and signaling by the focal adhesion targeting domain. *Structure* 10(3):319-327.
18. Gao G, *et al.* (2004) NMR solution structure of the focal adhesion targeting domain of focal adhesion kinase in complex with a paxillin LD peptide: evidence for a two-site binding model. *J Biol Chem* 279(9):8441-8451.
19. Hayashi I, Vuori K, & Liddington RC (2002) The focal adhesion targeting (FAT) region of focal adhesion kinase is a four-helix bundle that binds paxillin. *Nat Struct Biol* 9(2):101-106.
20. Cooper LA, Shen TL, & Guan JL (2003) Regulation of focal adhesion kinase by its amino-terminal domain through an autoinhibitory interaction. *Mol Cell Biol* 23(22):8030-8041.
21. Lietha D, *et al.* (2007) Structural basis for the autoinhibition of focal adhesion kinase. *Cell* 129(6):1177-1187.
22. Schaller MD, *et al.* (1994) Autophosphorylation of the focal adhesion kinase, pp125FAK, directs SH2-dependent binding of pp60src. *Mol Cell Biol* 14(3):1680-1688.
23. Toutant M, *et al.* (2002) Alternative splicing controls the mechanisms of FAK autophosphorylation. *Mol Cell Biol* 22(22):7731-7743.
24. Calalb MB, Polte TR, & Hanks SK (1995) Tyrosine phosphorylation of focal adhesion kinase at sites in the catalytic domain regulates kinase activity: a role for Src family kinases. *Mol Cell Biol* 15(2):954-963.
25. Schaller MD & Parsons JT (1995) pp125FAK-dependent tyrosine phosphorylation of paxillin creates a high-affinity binding site for Crk. *Mol Cell Biol* 15(5):2635-2645.
26. Tachibana K, *et al.* (1997) Tyrosine phosphorylation of Crk-associated substrates by focal adhesion kinase. A putative mechanism for the integrin-mediated tyrosine phosphorylation of Crk-associated substrates. *J Biol Chem* 272(46):29083-29090.
27. Frame MC, Patel H, Serrels B, Lietha D, & Eck MJ (2010) The FERM domain: organizing the structure and function of FAK. *Nat Rev Mol Cell Biol* 11(11):802-814.
28. Chen SY & Chen HC (2006) Direct interaction of focal adhesion kinase (FAK) with Met is required for FAK to promote hepatocyte growth factor-induced cell invasion. *Mol Cell Biol* 26(13):5155-5167.
29. Plaza-Menacho I, *et al.* (2011) Focal adhesion kinase (FAK) binds RET kinase via its FERM domain, priming a direct and reciprocal RET-FAK transactivation mechanism. *J Biol Chem* 286(19):17292-17302.
30. Sieg DJ, *et al.* (2000) FAK integrates growth-factor and integrin signals to promote cell migration. *Nat Cell Biol* 2(5):249-256.
31. Cai X, *et al.* (2008) Spatial and temporal regulation of focal adhesion kinase activity in living cells. *Mol Cell Biol* 28(1):201-214.
32. Goksoy E, *et al.* (2008) Structural basis for the autoinhibition of talin in regulating integrin activation. *Mol Cell* 31(1):124-133.
33. Palmer SM, Playford MP, Craig SW, Schaller MD, & Campbell SL (2009) Lipid binding to the tail domain of vinculin: specificity and the role of the N and C termini. *J Biol Chem* 284(11):7223-7231.
34. Legate KR, *et al.* (2011) Integrin adhesion and force coupling are independently regulated by localized PtdIns(4,5)2 synthesis. *EMBO J* 30(22):4539-4553.
35. McNamee HP, Liley HG, & Ingber DE (1996) Integrin-dependent control of inositol lipid synthesis in vascular endothelial cells and smooth muscle cells. *Exp Cell Res* 224(1):116-122.
36. Di Paolo G, *et al.* (2002) Recruitment and regulation of phosphatidylinositol phosphate kinase type 1 gamma by the FERM domain of talin. *Nature* 420(6911):85-89.
37. Ling K, Doughman RL, Firestone AJ, Bunce MW, & Anderson RA (2002) Type I gamma phosphatidylinositol phosphate kinase targets and regulates focal adhesions. *Nature* 420(6911):89-93.
38. Balabin IA, Yang W, & Beratan DN (2009) Coarse-grained modeling of allosteric regulation in protein receptors. *Proc Natl Acad Sci U S A* 106(34):14253-14258.
39. Wang Y, *et al.* (2013) Platelets lacking PIP5KIgamma have normal integrin activation but impaired cytoskeletal-membrane integrity and adhesion. *Blood* 121(14):2743-2752.
40. Kanchanawong P, *et al.* (2010) Nanoscale architecture of integrin-based cell adhesions. *Nature* 468(7323):580-584.
41. Schlessinger J (2000) Cell signaling by receptor tyrosine kinases. *Cell* 103(2):211-225.
42. Fabry B, Klemm AH, Kienle S, Schaffer TE, & Goldmann WH (2011) Focal adhesion kinase stabilizes the cytoskeleton. *Biophys J* 101(9):2131-2138.
43. Grant BD & Adams JA (1996) Pre-steady-state kinetic analysis of cAMP-dependent protein kinase using rapid quench flow techniques. *Biochemistry* 35(6):2022-2029.
44. Taylor SS, Keshwani MM, Steichen JM, & Kornev AP (2012) Evolution of the eukaryotic protein kinases as dynamic molecular switches. *Philos Trans R Soc Lond B Biol Sci* 367(1602):2517-2528.
45. Ritt M, Guan JL, & Sivaramakrishnan S (2013) Visualizing and manipulating focal adhesion kinase regulation in live cells. *J Biol Chem* 288(13):8875-8886.
46. Chen TH, Chan PC, Chen CL, & Chen HC (2011) Phosphorylation of focal adhesion kinase on tyrosine 194 by Met leads to its activation through relief of autoinhibition. *Oncogene* 30:153-166.
47. Sun Y, Ling K, Wagoner MP, & Anderson RA (2007) Type I gamma phosphatidylinositol phosphate kinase is required for EGF-stimulated directional cell migration. *J Cell Biol* 178(2):297-308.